

Blue whales (*Balaenoptera musculus*) optimize foraging efficiency by balancing oxygen use and energy gain as a function of prey density

Elliott Lee Hazen,^{1,2*} Ari Seth Friedlaender,^{3,4} Jeremy Arthur Goldbogen⁵

2015 © The Authors, some rights reserved; exclusive licensee American Association for the Advancement of Science. Distributed under a Creative Commons Attribution NonCommercial License 4.0 (CC BY-NC). 10.1126/sciadv.1500469

Terrestrial predators can modulate the energy used for prey capture to maximize efficiency, but diving animals face the conflicting metabolic demands of energy intake and the minimization of oxygen depletion during a breath hold. It is thought that diving predators optimize their foraging success when oxygen use and energy gain act as competing currencies, but this hypothesis has not been rigorously tested because it has been difficult to measure the quality of prey that is targeted by free-ranging animals. We used high-resolution multisensor digital tags attached to foraging blue whales (*Balaenoptera musculus*) with concurrent acoustic prey measurements to quantify foraging performance across depth and prey density gradients. We parameterized two competing physiological models to estimate energy gain and expenditure based on foraging decisions. Our analyses show that at low prey densities, blue whale feeding rates and energy intake were low to minimize oxygen use, but at higher prey densities feeding frequency increased to maximize energy intake. Contrary to previous paradigms, we demonstrate that blue whales are not indiscriminate grazers but instead switch foraging strategies in response to variation in prey density and depth to maximize energetic efficiency.

INTRODUCTION

Understanding how animals balance energy gain and metabolic expenditure is a central challenge of physiological ecology. Optimal foraging theory typically predicts the maximization of a single currency, such as the proportion of time spent on foraging, energy gain, or energetic efficiency (1–3). To maximize performance, particulate feeders that target single prey items are predicted to increase time spent on foraging as a function of increased prey patch quality (2, 4). However, terrestrial grazers, which are often categorized as batch or bulk foragers, have physiological limitations that influence handling and digestion times, thereby resulting in foraging strategies that prioritize time minimization foraging strategies relative to energy maximization (5). Some marine suspension-feeding vertebrates, such as baleen whales (Mysticeti), have been likened to terrestrial grazers (6, 7), where the combination of large body size and feeding in bulk on low-trophic level resources yields an energetically efficient foraging strategy (8). Although many whales feed on zooplankton or fish, their ancestry and digestive physiology (for example, multichambered stomachs and specialized bacteria) support the prevailing hypothesis that baleen whales are functionally convergent with terrestrial grazing herbivores (7). The most recent radiation of gigantic marine suspension feeders is represented by several baleen whale lineages (Mysticeti) (9), the largest of which include several rorqual species that exhibit an extreme lunge filter-feeding strategy whereby large volumes of prey-laden water are intermittently engulfed and filtered.

In contrast to particulate-feeding toothed whales (Odontoceti), baleen whales exhibit several modes of bulk filter feeding, ranging from

continuous ram filter feeding (bowhead and right whales, Balaenidae) to intermittent engulfment feeding (rorqual whales, Balaenopteridae). Balaenids swim at slow steady speeds to drive prey-laden water into the mouth (10), whereas rorquals accelerate forward in a rapid lunge to engulf discrete mouthfuls of targeted prey patches (8). Lunge filter feeding in rorquals is facilitated by a complex suite of morphological and biomechanical adaptations that enhance the extensibility of the throat pouch (11). Because of the acceleration and high drag associated with engulfment, the energetic cost of lunge feeding is predictably very high, estimated up to 50 times the basal metabolic rate for a similarly sized terrestrial mammal (12). Lunge feeding is a high-cost, high-benefit foraging mode that confers high energetic efficiency when engulfing very dense prey patches (8). However, the average densities of zooplankton over broad spatial scales are often several orders of magnitude below the critical threshold required to support the body size of the largest whales (13, 14). Therefore, rorquals must target dense and often deep prey patches for high prey intake and efficient foraging; otherwise, the energetic cost of lunge feeding will greatly exceed the energy gained from the captured prey (8).

Because rorqual whales are air-breathing divers that exhibit a high-cost feeding mechanism, they are under considerable pressure to optimize their foraging success when oxygen use and energy gain act as competing currencies (15). Longer dives require extended oxygen recovery time at the sea surface, thereby increasing the energy cost of a dive per unit time and decreasing the amount of time devoted to foraging at depth (16, 17). The prevailing hypothesis is that foraging behavior is primarily modulated by oxygen use, such that dive duration and lunge frequency are reduced to minimize the amount of oxygen expended and resultant surface recovery time, which we have termed the oxygen conservation strategy (1, 17, 18). In contrast, we hypothesize a threshold response, such that at low prey densities air-breathing foragers will exhibit low feeding rates and short dive durations to conserve oxygen, whereas at high prey densities feeding rates should increase to maximize energy gain. The trade-off between an energy-maximizing strategy (extended dive duration, increased feeding rate, and increased

¹Environmental Research Division/Southwest Fisheries Science Center/National Marine Fisheries Service/National Oceanic and Atmospheric Administration, Monterey, CA 93940, USA. ²Department of Ecology and Evolutionary Biology, University of California, Santa Cruz, Santa Cruz, CA 94923, USA. ³Marine Mammal Institute, Hatfield Marine Science Center, Oregon State University, Newport, OR 97365, USA. ⁴Southall Environmental Associates, Aptos, CA 95003, USA. ⁵Department of Biology, Hopkins Marine Station, Stanford University, Pacific Grove, CA 93950, USA.

*Corresponding author. E-mail: elliot.hazen@noaa.gov

oxygen consumption) compared to an oxygen-conserving strategy (shortened dive duration, decreased feeding rate, and decreased oxygen consumption) is diagrammed in Fig. 1. We tested this hypothesis

in the largest lunge filter feeder, the blue whale (*Balaenoptera musculus*), because they are extremely dependent on dense krill patches for energetically efficient foraging (8). By using concurrent foraging and prey

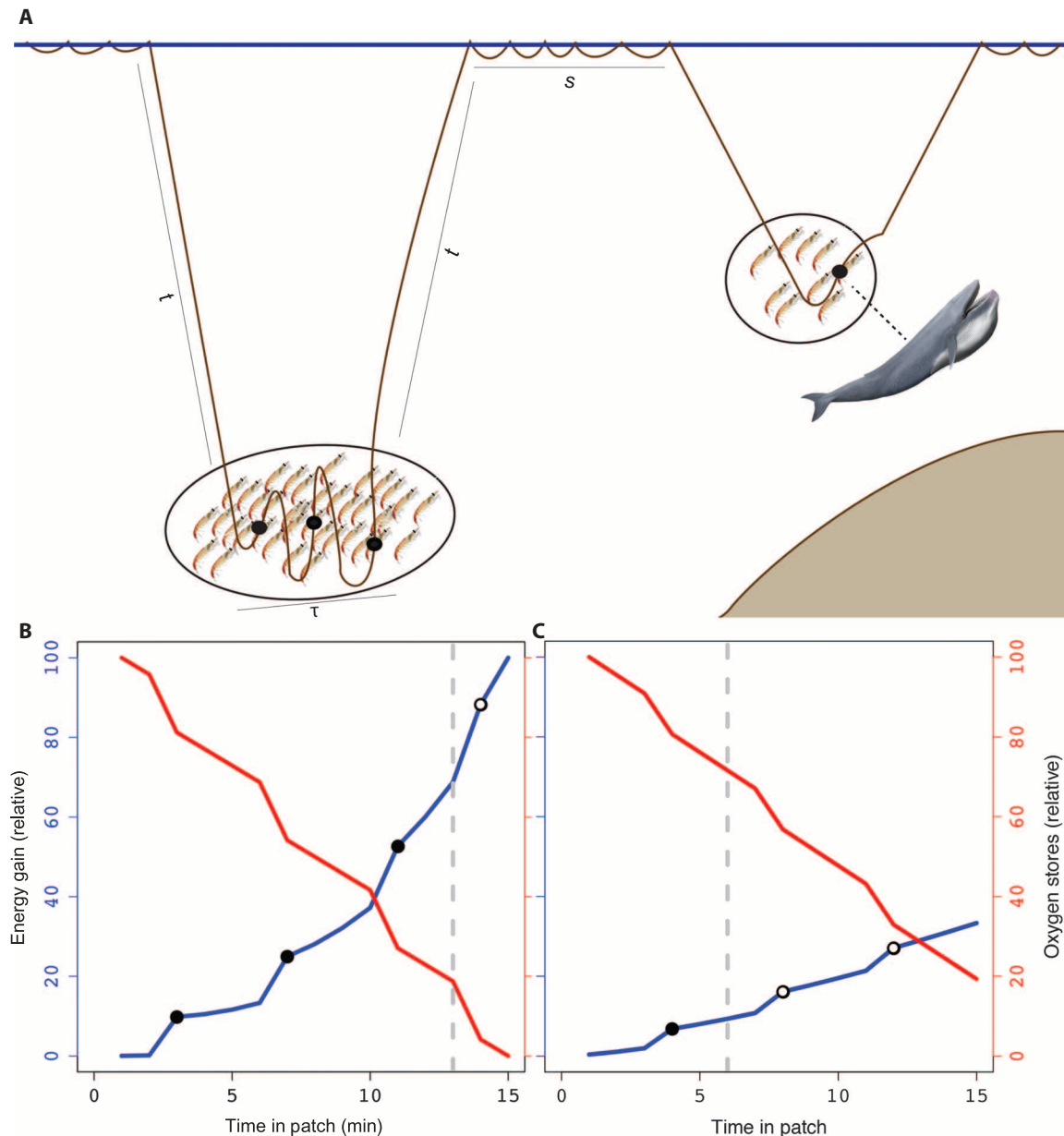


Fig. 1. Theoretical response of blue whale diving-foraging performance as a function of prey density and depth on high-density (left) and low-density (right) density prey patches. (A) Portions of an individual's dive are referenced by equation parameters including dive time (t), bottom time (τ), surface time (s), and number of lunges (L) marked with black circles. Recovery time at the surface increases greater than a 1:1 relationship with oxygen use; thus, conservation strategies significantly decrease time spent at the surface. (B and C) Foraging on two prey patches that vary in density and depth demonstrates the trade-off between the two approaches. Solid black points show hypothetical lunges, hollow white points show abandoned lunges (for example, the dive is aborted before these lunges are performed), and the dashed gray line shows the time at which the whale aborted the foraging dive. The two foraging scenarios illustrate the difference between the strategies (B) maximizing energy gain by increasing lunges per dive at the expense of oxygen when prey density is high and (C) minimizing oxygen use by decreasing lunges per dive. The blue line shows relative energy gain, whereas the red line shows hypothetical oxygen stores termed the theoretical aerobic dive limit (TADL). The blue line shows relative energy gain, whereas the red line shows the oxygen use, demonstrating the trade-off between oxygen and energy when feeding at depth. Energy gain is greater per lunge when foraging on dense prey, but lunge costs remain the same. To optimize foraging efficiency (energy gain relative to energy used), when dense prey patches are available, we hypothesize that a whale will perform more lunges resulting in (i) a longer dive, (ii) more energy gained, and (iii) more oxygen consumed (B). This differs from a low-density prey scenario, where minimizing oxygen use while foraging is more important than maximizing energy gain (C).

data, we show that blue whales modulate their feeding rates to optimize energetic efficiency as a function of prey patch depth and density.

RESULTS

The feeding performance of tagged blue whales widely varied as a function of prey density and distribution. We analyzed tag data from 55 adult blue whales: 14 blue whales with concurrent prey measurements from 2011 to 2013 off the coast of California and 41 blue whales without prey from 2001 to 2010 (8, 19). Tag data with temporally and spatially coincident prey data included 374 foraging dives and 631 lunge-feeding events. The maximum depth of foraging dives ranged from 41 to 310 m, and dive times were 0.4 to 15.9 min in duration. Krill patch densities averaged across blue whale foraging bouts varied from 30 to 550 krill m^{-3} at depths of 55 to 360 m. The tag data showed that maximum lunge frequency (defined as the greatest number of lunges observed per dive for each whale) was greatest at about 280 m in depth, followed by a secondary peak in maximum lunges per dive at 115 m (Fig. 2). The greatest number of krill patches was found at depths between 115 and 235 m, but krill density was highest (>200 krill m^{-3}) between 110 and 175 m with a secondary peak at 305 m.

The total number of lunges per depth bin and the average number of lunges per dive both positively correlated with prey density ($R^2 = 0.24$ and 0.25 , respectively) and the number of prey patches ($R^2 = 0.12$ and 0.29 , respectively). We found that blue whales foraging on low krill densities fed at low rates (two to three lunges per dive), aligning

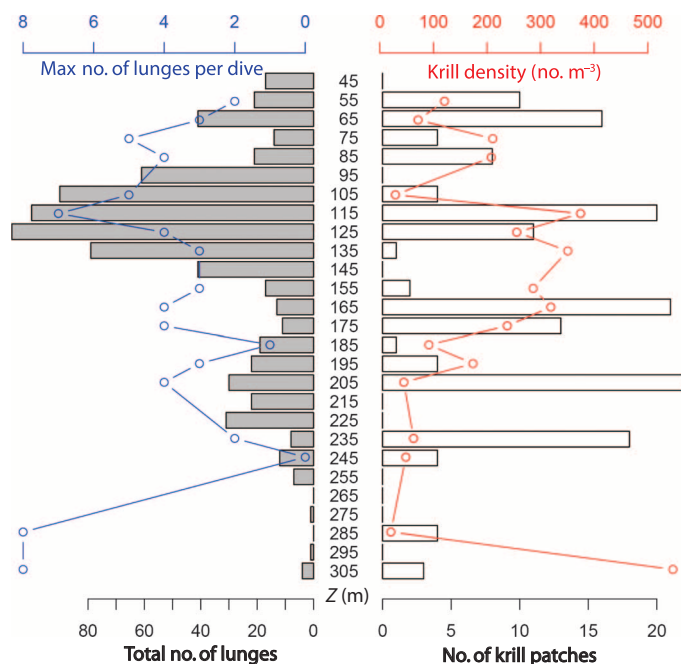


Fig. 2. Vertical partitioning of feeding lunges and prey. Whale foraging parameters (left) and krill patch metrics (right) are plotted with common depths on the y axis from 2011 to 2013 individuals. The total number of lunges across all whales (gray bars) and maximum number of lunges per dive (blue) are shown on the left, whereas the number of krill patches by centroid depth bin (white) and krill density per patch (red) are shown on the right. Both the number of patches and krill density are important metrics to understand dive behavior of foraging blue whales.

with the predicted oxygen-conserving strategy, but increased their feeding rates (four to eight lunges per dive) when foraging on denser patches (Fig. 3). Most tagged whales performed foraging dives within their predicted aerobic capacity (TADL), but a few individuals incurred an oxygen debt to extend foraging times on dense krill patches. Although it may be a continuum, the blue whales appeared to switch between oxygen-conserving and energy-maximizing foraging strategies as a function of krill density (Fig. 3A). This shift in diving behavior was predicted to occur at 175 krill m^{-3} [95% confidence interval (CI), 81 to 245 krill m^{-3}], although no krill patches were measured between 100 and 200 krill m^{-3} (Fig. 3B; $R^2 = 0.66$). Our analyses suggest that these two strategies (oxygen minimization and energy maximization) result in a divergence in efficiency at a prey density threshold of ~ 100 krill m^{-3} , above which increasing feeding rates to maximize energy gained was more efficient than lowering feeding rates to minimize oxygen use [Fig. 3C; slopes significantly different, ANCOVA $P < 0.001$].

DISCUSSION

Our results indicate that foraging blue whales minimize oxygen use by decreasing the number of lunges per dive when feeding on low-density krill patches. In contrast, blue whales maximized energy intake, at the expense of high oxygen use, by increasing lunge-feeding rates when targeting dense krill patches. Optimal foraging theory predicts that an animal should remain in a patch as long as energy gain is greater than the cost of foraging (3). However, this principle does not reflect the need to optimize multiple components of foraging, including the rate of energy gain, movement costs, time minimization, and energetic efficiency (20). An additional challenge for air-breathing marine predators is that they often perform deep dives in search of prey, and must decide whether to reduce foraging effort to conserve oxygen consumption or increase feeding rates to maximize energy gain (2, 4). Although we have tested two explicit hypotheses related to oxygen conservation and energy maximization, our study shows that these two processes are not mutually exclusive and that animals may seek to optimize both for maximum overall energy efficiency.

The principles of optimal foraging theory have been tested in controlled environments for terrestrial and marine organisms (4, 21), but rarely have these relationships been examined in the wild (22–24). Dive duration, dive depth, and surface time for air-breathing predators are often correlated, such that a deeper dive results in longer foraging bouts and increased recovery at the sea surface (1). Oxygen has been shown to act as a constraint on foraging time in amphibious mammals, where surface search methods resulted in longer dives compared to those at depth when prey was constant, termed the “aqualung effect” (25). Models have predicted that air-breathing diving animals will remain in a prey patch longer when patch quality is higher, and deeper dives are less likely to be terminated as a function of prey quality (2, 26). However, field tests with particulate feeders have shown equivocal results, where patch departure differed from theory based on patch quality predictions or time spent foraging (20, 23, 24, 27). For large grazing ungulates such as wood bison (*Bison bison athabasca* Rhoads), the relationship between patch residence time and patch quality is more robust, where individuals fit a time-minimizing model more often than an energy maximization model (5). For diving pinnipeds, the relationship between dive duration and prey availability is more complex. Harbor

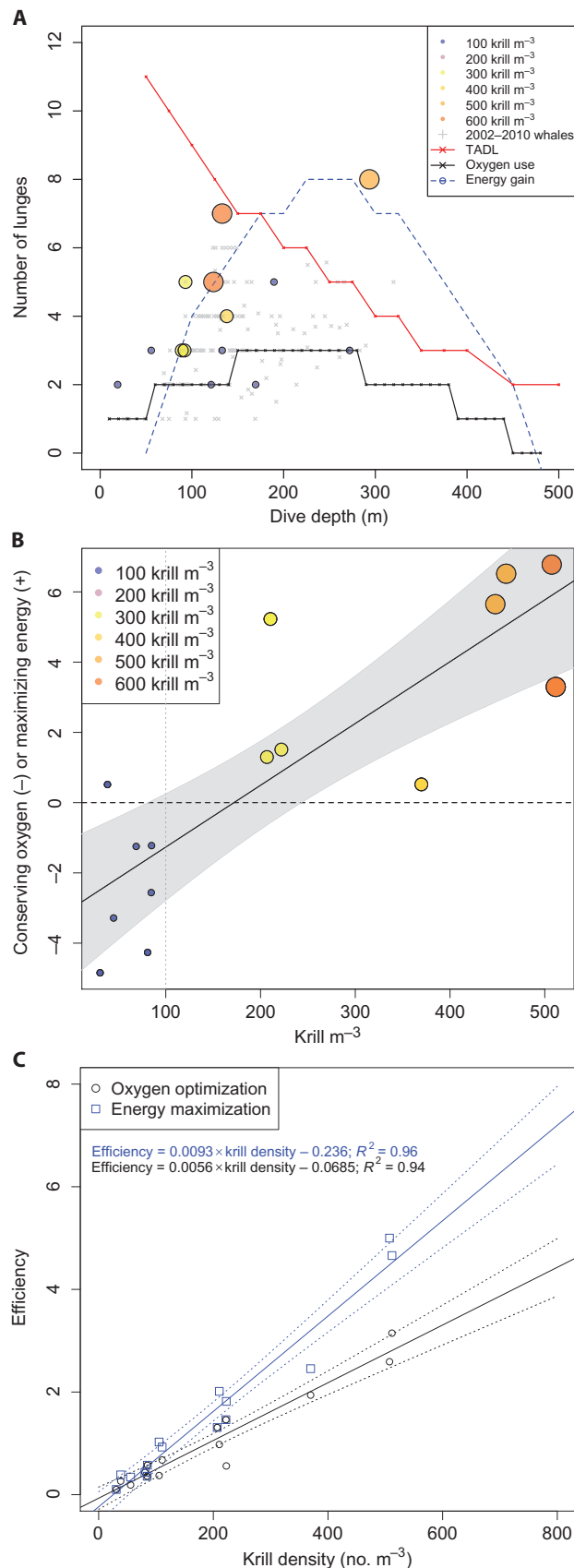
Fig. 3. Blue whale optimal foraging behaviors relative to krill density.

(A) Predicted number of lunges as a function of dive depth based on models of energy gain (blue dashed line) and oxygen conservation (black line). The estimated TADL for a 22-m whale, the point at which an individual goes hypoxic, is shown in red (8). The maximum number of lunges per dive with concurrent measured krill densities (size and color of circles) are plotted against dive depth ($n = 14$ whales). Historical maximum lunges per dive ($n = 41$ whales) that were collected in the absence of prey measurements are plotted with gray symbols. (B) The difference in residuals ($\text{residuals}_{\text{Eq. 2}} - \text{residuals}_{\text{Eq. 1}}$) between maximum lunges per individual whale and the two foraging models shows the point at which individuals switch from maximizing energy (positive) to conserving oxygen (negative; $R^2 = 0.66$). The reference of 100 krill m^{-3} below which it has been hypothesized to be energetically inefficient to forage (8) is shown in dashed gray line. CIs (95%) are shaded in gray. (C) Efficiency rates, the ratio of the energy gained divided by all energy expenditures, estimated on actual krill density measurements using both foraging models (oxygen use and energy gain) are shown in black circles and blue squares, respectively. The two efficiencies have significantly different slopes [analysis of covariance (ANCOVA), $P < 0.001$]. CIs (95%) around both models are represented by dotted lines.

seals (*Phoca vitulina concolor*) spent more time at depth when prey encounter rate was low (28). In contrast, southern elephant seals (*Mirounga leonina*) aborted dives earlier when prey concentrations were low over broad spatial scales (20). The distinction between these two predators may correspond to the difference in their maximum dive depths and need for oxygen conservation on long dives, similar to blue whales shown here. The novelty of our findings is that we empirically show that blue whales switch between time-minimizing and energy-maximizing foraging strategies as a function of prey density. Therefore, we suggest that the flexibility of these foraging strategies allows blue whales to optimize their energy gain from patchy and ephemeral resources over broader spatiotemporal scales and thus maintain their large body size.

The observed foraging behavior in this study showed a strong delineation between individuals conserving oxygen when prey density was less than 100 krill m^{-3} and other individuals maximizing energy gain when prey density was greater than 200 krill m^{-3} (Fig. 3B). These data support previous estimates of the minimum prey densities of 100 krill m^{-3} required to maintain the basic energetic demands of blue whales (8), but we also observed a baseline foraging effort of one to three lunge-feeding events per dive on lower densities of prey. This low feeding rate may be a mechanism used by whales to assess prey density on a dive-by-dive basis so that whales can respond quickly and increase feeding rates when dense krill patches are encountered at depth. The cost of lunge feeding is so high that blue whales must locate and exploit krill patches that are greater than 100 krill m^{-3} to support not only maintenance costs but also the ability to acquire an energetic surplus for migration and reproduction (8, 29). Here, we show that blue whales are able to target high-density krill aggregations and respond to these high-quality prey patches by increasing feeding rates to maximize efficiency.

Our estimates of energetic efficiency, defined as the ratio of the energy gained from assimilated prey to the energy expended during foraging, suggest that blue whales were able to double their foraging efficiency by increasing lunge-feeding rates on high-density krill patches (Fig. 3C). However, at low krill densities ($\sim 100 \text{ krill m}^{-3}$), our efficiency estimates for these two predictions converge, suggesting that modulating feeding rate will have little effect on foraging efficiency when prey patch quality is low. It is unknown how bulk filter feeders detect prey



aggregations in the open ocean, but research suggests that physical cues such as oceanographic fronts play a major role in guiding search behavior in basking sharks (30). At similarly broad scales, blue whales may use past memory and social cues to find persistent hot spots (31), but at fine scales, they likely use multiple sensory modalities to assess prey density, from visual cues to mechanosensory feedback, after the first lunge-feeding event of a given dive of a foraging bout (32). Because lunge feeding is energetically costly, an increase in feeding rate on low-density prey patches will cost more energy relative to that of assimilated prey. Thus, we posit that the low feeding rate foraging strategy allows blue whales to assess the prey field while conserving oxygen as predicted by optimal foraging theory. Such a strategy may allow blue whales to have greater aerobic capacity to devote to longer dives when high-quality prey patches are encountered at depth.

Collectively, our analyses clarify the behavioral scope and energetic niche available to blue whales across patchy and heterogeneous prey fields. Our results demonstrate that blue whales are not indiscriminant grazers as previously depicted (6, 7), but rather their intermittent bulk filter-feeding strategy enables the efficient exploitation of discrete patches of dense prey (7). Although we examined the dive-by-dive scale of foraging decisions, we currently lack an understanding of how feeding performance varies across broader seasonal and annual time scales, ultimately translating to population dynamics. Although blue whales may expend more energy per lunge with increased maneuvering when foraging on a less-dense prey patch (32), the high efficiency when foraging on dense prey patches is likely critical in maintaining a long-term energetic surplus. By maximizing efficiency while feeding, blue whales can satisfy the tremendous energetic demands required of their large body size and reproductive biology. Efficient foraging facilitates the development of massive lipid reserves required for long-distance fasting during migrations to low-latitude breeding grounds (8, 31, 33). This life history strategy is common in many gigantic bulk filter feeders that exhibit an ecomorphology that confers a low energetic cost of transport across ocean basins and high-energy intake during brief seasonal foraging bouts (34).

A large body size reflects successful strategies to maximize energy intake while simultaneously minimizing the costs associated with foraging (6, 35). Among all the gigantic terrestrial grazers and marine suspension feeders, rorquals are unique in that their bulk-feeding mode is intermittent. Compared to “marine grazing,” or continuous ram filter feeding that is exemplified by Balaenid whales [bowhead whales (*Balaena mysticetus*) and right whales (*Eubalaena* sp.)] and basking sharks (*Cetorhinus maximus*) (36, 37), lunge feeding in rorqual whales is predictably more efficient at consuming a patchy resource. Lunge feeding allows for rapid prey patch engulfment and increased patch-switching ability because rorquals exhibit an increased engulfment capacity relative to the duration of engulfment. For example, a blue whale can engulf about 80 m³ of prey-laden water in 7 s, whereas a continuously ram-feeding bowhead whale would require 25 s to filter the same target volume (38). Blue whale lunge-feeding speeds of up to 5 m s⁻¹ greatly exceed the escape speeds of krill (<1 m s⁻¹) (39), and a blue whale could therefore consume an entire 80-m³ prey patch in a single gulp compared to several slow-moving passes (~1 m s⁻¹) that would be required by a continuous ram feeder (10, 38). However, continuous ram filter feeding is predictably less costly than intermittent lunge feeding because of low swimming speeds and hydrodynamic mechanisms associated with the engulfment apparatus that may decrease drag during foraging (37). As a consequence, continuous ram filter feeders may

exhibit lower threshold biomass densities compared to intermittent filter-feeding rorqual whales (36, 40).

As blue whales represent an extreme in rorqual size and physiology, smaller rorqual species may have different behavioral strategies that maximize foraging efficiency. For example, humpback whales and fin whales often feed on krill sympatric with blue whales (14, 41) yet can also target fish. This approach allows them to remain longer in a foraging location but may not offer the energetic efficiency that krill specialization strategies likely confer (8, 12, 14). Given that krill are seasonally recurrent, yet are inherently patchy prey resources in many ecosystems, this pairing of krill specialization with an intermittent engulfment mechanism results in optimized efficiency in foraging behaviors and supports the energetic demand required by the large-bodied blue whales. However, quantifying and rigorously testing the mechanisms that large, free-ranging predators use to successfully forage has been difficult to demonstrate experimentally in the open ocean. Our results provide evidence of how the combination of morphological specialization and behavioral plasticity shapes the foraging energetics and functional ecology of the largest predators.

METHODS

Tag data

We used noninvasive, high-resolution, digital acoustic recording archival tags (DTAGs) to investigate the feeding behavior and ecological decision-making of foraging blue whales. The 7-m rigid-hulled inflatable tag boat approaches the whale from the rear (often on the last breath of a surfacing sequence in between longer dives), deploys the suction cup tag using a 6-m carbon-fiber pole, and then quickly moves away from the whale (38). The DTAG is programmed to release from the whale using an electric corrosive release that floods the suction cups, floats to the surface, and is located via an onboard acoustic very high frequency transmitter.

DTAGs contain a sensor suite that includes a pressure transducer, triaxial accelerometers and magnetometers that allow the measurement of fine-scale foraging behavior under the surface, and embedded stereo hydrophones (42). All DTAGs were calibrated before deployment (42), and upon recovery, the sensor data were downloaded and analyzed. All auxiliary sensor channels were sampled at 50 Hz but were decimated to 5 Hz in post-processing. The orientation of the whale, swimming strokes, and acceleration rate of change (that is, “jerk”) were calculated from the raw accelerometer signals and used to identify individual feeding lunges (19). The data were collected during SOCAL (Southern California) behavioral response studies (43), but all data during and within 1 hour of sound exposure were not included in this study. We examined historical dive data from 2001 to 2010 ($n = 41$) from DTAG and Bioacoustic Probe deployments (8, 19, 44) collected in the coastal waters of southern California without prey measurements and DTAG deployments on blue whales from 2011 to 2013 ($n = 14$) that included concurrent measurements of prey.

Prey data

We quantified the prey field in the vicinity (<1 km) of tagged blue whales using dual-frequency Simrad EK60 echo sounders (38 and 120 kHz) (45) that were calibrated following standardized methods (46). The acoustic backscatter was sampled at 10 Hz with pulse widths of 512 and 256 μ s for the 38- and 120-kHz beams at 12° and 7° width, respectively, thereby measuring acoustic density [scattering volume

(S_V) for specific prey patches. The echo sounders were continuously towed between 2 and 5 knots in a clover leaf sampling design protocol to measure anisotropy in prey patch size (45). Mapped prey schools were detected using the SHAPES (Shoal Analysis and Patch Estimation System) school detection algorithm (5-m linking distance) within Echoview 5 (www.myriax.com) incorporating a -75 -dB threshold. We used net tow samples, combined with published krill size distributions, to calculate a mean adult krill length of 28 mm in this region (47). We calculated an estimate of krill target strength of -75 dB based on mean lengths described above and published target strength-length relationships to estimate krill density in grams per cubic meter of seawater (47). Krill target strength estimates and acoustic patch densities were used to convert acoustic backscatter to estimates of krill density (no. m^{-3}) (46). We also examined the difference in scattering between the 120- and 38-kHz acoustic data to ensure that schools were consistent with krill scattering properties. For each krill patch that was detected, we measured krill density, patch height, and mean patch depth. We calculated the position of the tagged whales during each surfacing series using a laser range finder and Global Positioning System and only used data for prey patches that were <1 km from foraging whales for further analyses.

Foraging equations

We used two equations to examine the trade-off between oxygen conservation and energy gain (18, 26). The oxygen conservation equation calculates foraging duration as a function of minimizing surface time, whereas the energy-maximizing equation calculates foraging duration as a function of patch density. We parameterized the relationship of oxygen use as a function of diving using estimates summarized by Doniol-Valcroze *et al.* (18) and revised the energetic cost estimates from Potvin *et al.* (12) to generate metabolic rates for each component of a blue whale dive. Potvin *et al.* (12) reported lunges lasting 80 s for blue whales, which result in an estimated energetic cost of 343.98 kJ (17.1 liters of O_2). These values were compared to previously published estimates to examine the range of energetic parameterization for blue whales, and the most conservative estimates were used in comparing the two strategies. Houston and Carbone's (1) equation of oxygen use was able to incorporate specific behavioral costs (for example, engulfment metabolic rate, basal metabolic rate, and prey approach metabolic rate; table S1) (12). Oxygen use is calculated as a trade-off between surface oxygen repletion, storage, and behavioral costs (dive and lunge; Eq. 1). Because surface time increases nonlinearly with oxygen depletion, minimizing oxygen use results in a significant time reduction between foraging bouts (17)

$$K(1 - e^{-\alpha s}) = m_1 \tau + m_2 t \quad (1)$$

where K is the total oxygen storage (liters of O_2), α is the rate of oxygen replenishment (liters of $\text{O}_2 \cdot \text{s}^{-1}$), s is the surface time (seconds) versus m_1 (forage costs; liters of $\text{O}_2 \cdot \text{s}^{-1}$), τ is the forage time (seconds), m_2 is the travel cost (liters of $\text{O}_2 \cdot \text{s}^{-1}$), and t is the travel time (seconds).

Energetic gain was modeled using a simple equation as a function of time spent foraging, patch quality, and an energy conversion factor (Eq. 2) (26)

$$g = a \cdot t^x \quad (2)$$

where g is the energy intake (kJ s^{-1}), a is the energy conversion factor (kJ), t is the time in patch (seconds), and x is the patch quality (unitless).

For the energy gain model, we examined the average patch quality (krill density) compared to the maximum patch quality measured across all whales rather than fitting the equation to individual whales or patches. This averaged approach allowed us to test the dive behavior of each whale against two competing models. Historical dive data without prey data were included to examine broader patterns in the context of these model predictions. Our results were limited to examining a single best-fit form of the gain function (second-order polynomial) rather than multiple potential forms of the equation (22). We used individual lunges as a discrete metric of feeding performance, given that rorqual whales exhibit a clear kinematic signature during lunge feeding (19) that is not easily discerned in other animals.

The maximum number of lunges per dive for each whale was used as the common currency among energy use and oxygen consumption. We also estimated TADL, the length of a dive at which a blue whale would transition from aerobic to anaerobic oxygen use, based on previously published equations (8). These equations were plotted with depth on the x axis and the predicted number of lunges on the y axis. The residuals between theory (as predicted by Eqs. 1 and 2) and observed feeding performance were subtracted from each other (residual difference = $\text{residuals}_{\text{Eq. 2}} - \text{residuals}_{\text{Eq. 1}}$) to examine whether individual foraging dive decisions conformed more closely to conserving oxygen (Eq. 1) or to maximizing energy gain (Eq. 2). Positive values indicate that the number of lunges per dive more closely aligns with an energy-maximizing approach, whereas negative values indicate closer alignment with an oxygen conservation strategy. The intercept of the linear regression represents the threshold between these two foraging strategies. We combined the energetic expenditures of diving, lunge feeding, filtering, and surface recovery time (12) as an estimate of total dive cost, with lunges predicted by the oxygen conservation and energy gain based models. The energetic efficiency of foraging was calculated using a ratio of energy gain per dive divided by the costs associated with the foraging described above (8). These methods provide a range of parameters for oxygen use estimation for North Pacific blue whales and a calibrated energy gain equation to quantify observed foraging strategies relative to prey patch density and depth.

SUPPLEMENTARY MATERIALS

Supplementary material for this article is available at <http://advances.sciencemag.org/cgi/content/full/1/9/e1500469/DC1>

Table S1. Reparameterization of equations used in optimal foraging models from Houston and Carbone (1), Doniol-Valcroze *et al.* (18), and Mori *et al.* (26).

REFERENCES AND NOTES

1. A. I. Houston, C. Carbone, The optimal allocation of time during the diving cycle. *Behav. Ecol.* **3**, 255–265 (1992).
2. D. Thompson, M. A. Fedak, How long should a dive last? A simple model of foraging decisions by breath-hold divers in a patchy environment. *Anim. Behav.* **61**, 287–296 (2001).
3. R. H. MacArthur, E. R. Pianka, On optimal use of a patchy environment. *Am. Nat.* **100**, 603–609 (1966).
4. C. E. Sparling, J.-Y. Georges, S. L. Gallon, M. Fedak, D. Thompson, How long does a dive last? Foraging decisions by breath-hold divers in a patchy environment: A test of a simple model. *Anim. Behav.* **74**, 207–218 (2007).
5. C. M. Bergman, J. M. Fryxell, C. C. Gates, D. Fortin, Ungulate foraging strategies: Energy maximizing or time minimizing? *J. Anim. Ecol.* **70**, 289–300 (2001).
6. R. M. Sibly, J. H. Brown, Effects of body size and lifestyle on evolution of mammal life histories. *Proc. Natl. Acad. Sci. U.S.A.* **104**, 17707–17712 (2007).
7. T. M. Williams, in *Whales, Whaling, and Ocean Ecosystems*, J. A. Estes, D. P. DeMaster, D. F. Doak, T. M. Williams, R. L. Brownell Jr., Eds. (University of California Press, Berkeley, CA, 2006), pp. 191–201.

8. J. A. Goldbogen, J. Calambokidis, E. Oleson, J. Potvin, N. D. Pyenson, G. Schorr, R. E. Shadwick, Mechanics, hydrodynamics and energetics of blue whale lunge feeding: Efficiency dependence on krill density. *J. Exp. Biol.* **214**, 131–146 (2011).
9. T. A. Deméré, M. R. McGowen, A. Berta, J. Gatesy, Morphological and molecular evidence for a stepwise evolutionary transition from teeth to baleen in mysticete whales. *Syst. Biol.* **57**, 15–37 (2008).
10. M. Simon, M. Johnson, P. Tyack, P. T. Madsen, Behaviour and kinematics of continuous ram filtration in bowhead whales (*Balaena mysticetus*). *Proc. Biol. Sci.* **276**, 3819–3828 (2009).
11. N. D. Pyenson, J. A. Goldbogen, A. W. Vogl, G. Szathmari, R. L. Drake, R. E. Shadwick, Discovery of a sensory organ that coordinates lunge feeding in rorqual whales. *Nature* **485**, 498–501 (2012).
12. J. Potvin, J. A. Goldbogen, R. E. Shadwick, Metabolic expenditures of lunge feeding rorquals across scale: Implications for the evolution of filter feeding and the limits to maximum body size. *PLOS One* **7**, e44854 (2012).
13. P. F. Brodie, D. D. Sameoto, R. W. Sheldon, Population densities of euphausiids off Nova Scotia as indicated by net samples, whale stomach contents, and sonar. *Limnol. Oceanogr.* **23**, 1264–1267 (1978).
14. D. A. Croll, B. Marinovic, S. Benson, F. P. Chavez, N. Black, R. Ternullo, B. R. Tershy, From wind to whales: Trophic links in a coastal upwelling system. *Mar. Ecol. Prog. Ser.* **289**, 117–130 (2005).
15. J. A. Goldbogen, J. Calambokidis, D. A. Croll, M. F. McKenna, E. Oleson, J. Potvin, N. D. Pyenson, G. Schorr, R. E. Shadwick, B. R. Tershy, Scaling of lunge-feeding performance in rorqual whales: Mass-specific energy expenditure increases with body size and progressively limits diving capacity. *Funct. Ecol.* **26**, 216–226 (2012).
16. G. L. Kooyman, M. A. Castellini, R. W. Davis, Physiology of diving in marine mammals. *Annu. Rev. Physiol.* **43**, 343–356 (1981).
17. A. Acevedo-Gutiérrez, D. A. Croll, B. R. Tershy, High feeding costs limit dive time in the largest whales. *J. Exp. Biol.* **205**, 1747–1753 (2002).
18. T. Doniol-Valcroze, V. Lesage, J. Giard, R. Michaud, Optimal foraging theory predicts diving and feeding strategies of the largest marine predator. *Behav. Ecol.* **22**, 880–888 (2011).
19. J. A. Goldbogen, J. Calambokidis, A. S. Friedlaender, J. Francis, S. L. DeRuiter, A. K. Stimpert, E. Falcone, B. L. Southall, Underwater acrobatics by the world's largest predator: 360° rolling manoeuvres by lunge-feeding blue whales. *Biol. Lett.* **9**, 20120986 (2013).
20. M. Thums, C. J. A. Bradshaw, M. D. Sumner, J. M. Horsburgh, M. A. Hindell, Depletion of deep marine food patches forces divers to give up early. *J. Anim. Ecol.* **82**, 72–83 (2013).
21. P. Nonacs, State dependent behavior and the marginal value theorem. *Behav. Ecol.* **12**, 71–83 (2001).
22. Y. Y. Watanabe, M. Ito, A. Takahashi, Testing optimal foraging theory in a penguin–krill system. *Proc. Biol. Sci.* **281**, 20132376 (2014).
23. Y. Mori, I. L. Boyd, The behavioral basis for nonlinear functional responses and optimal foraging in Antarctic fur seals. *Ecology* **85**, 398–410 (2004).
24. I. L. Boyd, J. P. Y. Arnould, T. Barton, J. P. Croxall, Foraging behaviour of Antarctic fur seals during periods of contrasting prey abundance. *J. Anim. Ecol.* **63**, 703–713 (1994).
25. N. Dunstone, R. J. O'Connor, Optimal foraging in an amphibious mammal. I. The aqualung effect. *Anim. Behav.* **27**, 1182–1194 (1979).
26. Y. Mori, A. Takahashi, F. Mehlum, Y. Watanuki, An application of optimal diving models to diving behaviour of Brünnich's guillemots. *Anim. Behav.* **64**, 739–745 (2002).
27. J. C. Alonso, J. A. Alonso, L. M. Bautista, R. Muñoz-Pulido, Patch use in cranes: A field test of optimal foraging predictions. *Anim. Behav.* **49**, 1367–1379 (1995).
28. S. G. Heaslip, W. D. Bowen, S. J. Iverson, Testing predictions of optimal diving theory using animal-borne video from harbour seals (*Phoca vitulina concolor*). *Can. J. Zool.* **92**, 309–318 (2014).
29. J. Wiedenmann, K. A. Cresswell, J. Goldbogen, J. Potvin, M. Mangel, Exploring the effects of reductions in krill biomass in the Southern Ocean on blue whales using a state-dependent foraging model. *Ecol. Model.* **222**, 3366–3379 (2011).
30. P. I. Miller, K. L. Scales, S. N. Ingram, E. J. Southall, D. W. Sims, Basking sharks and oceanographic fronts: Quantifying associations in the north-east Atlantic. *Funct. Ecol.* **29**, 1099–1109 (2015).
31. H. Bailey, B. R. Mate, D. M. Palacios, L. Irvine, S. J. Bograd, D. P. Costa, Behavioural estimation of blue whale movements in the Northeast Pacific from state-space model analysis of satellite tracks. *Endang. Species Res.* **10**, 93–106 (2009).
32. J. A. Goldbogen, E. L. Hazen, A. S. Friedlaender, J. Calambokidis, S. L. DeRuiter, A. K. Stimpert, B. L. Southall, Prey density and distribution drive the three-dimensional foraging strategies of the largest filter feeder. *Funct. Ecol.* **29**, 951–961 (2015).
33. P. F. Brodie, Cetacean energetics, an overview of intraspecific size variation. *Ecology* **56**, 152–161 (1975).
34. D. W. Sims, E. J. Southall, N. E. Humphries, G. C. Hays, C. J. A. Bradshaw, J. W. Pitchford, A. James, M. Z. Ahmed, A. S. Brierley, M. A. Hindell, D. Morrill, M. K. Musyl, D. Righton, E. L. C. Shepard, V. J. Wearmouth, R. P. Wilson, M. J. Witt, J. D. Metcalfe, Scaling laws of marine predator search behaviour. *Nature* **451**, 1098–1102 (2008).
35. F. A. Smith, A. G. Boyer, J. H. Brown, D. P. Costa, T. Dayan, S. K. Morgan Ernest, A. R. Evans, M. Fortelius, J. L. Gittleman, M. J. Hamilton, L. E. Harding, K. Lintulaakso, S. Kathleen Lyons, C. McCain, J. G. Okie, J. J. Saarinen, R. M. Sibly, P. R. Stephens, J. Theodor, M. D. Uhen, The evolution of maximum body size of terrestrial mammals. *Science* **330**, 1216–1219 (2010).
36. D. W. Sims, M. J. Witt, A. J. Richardson, E. J. Southall, J. D. Metcalfe, Encounter success of free-ranging marine predator movements across a dynamic prey landscape. *Proc. Biol. Sci.* **273**, 1195–1201 (2006).
37. A. J. Werth, Models of hydrodynamic flow in the bowhead whale filter feeding apparatus. *J. Exp. Biol.* **207**, 3569–3580 (2004).
38. J. A. Goldbogen, A. S. Friedlaender, J. Calambokidis, M. F. McKenna, M. Simon, D. P. Nowacek, Integrative approaches to the study of baleen whale diving behavior, feeding performance, and foraging ecology. *BioScience* **63**, 90–100 (2013).
39. W. M. Hamner, Aspects of schooling in *Euphausia superba*. *J. Crustacean Biol.* **4**, 67–74 (1984).
40. S. E. Parks, J. D. Warren, K. Stamieszkin, C. A. Mayo, D. Wiley, Dangerous dining: Surface foraging of North Atlantic right whales increases risk of vessel collisions. *Biol. Lett.* **8**, 57–60 (2012).
41. A. S. Friedlaender, J. A. Goldbogen, E. L. Hazen, J. Calambokidis, B. L. Southall, Feeding performance by sympatric blue and fin whales exploiting a common prey resource. *Mar. Mamm. Sci.* **31**, 345–354 (2015).
42. M. P. Johnson, P. L. Tyack, A digital acoustic recording tag for measuring the response of wild marine mammals to sound. *IEEE J. Ocean. Eng.* **28**, 3–12 (2003).
43. J. A. Goldbogen, B. L. Southall, S. L. DeRuiter, J. Calambokidis, A. S. Friedlaender, E. L. Hazen, E. A. Falcone, G. S. Schorr, A. Douglas, D. J. Moretti, C. Kyburg, M. F. McKenna, P. L. Tyack, Blue whales respond to simulated mid-frequency military sonar. *Proc. Biol. Sci.* **280**, 20130657 (2013).
44. W. Burgess, P. Tyack, B. Le Boeuf, D. Costa, A programmable acoustic recording tag and first results from free-ranging northern elephant seals. *Deep Sea Res. Pt. II* **45**, 1327–1351 (1998).
45. E. L. Hazen, A. S. Friedlaender, M. A. Thompson, C. R. Ware, M. T. Weinrich, P. N. Halpin, D. N. Wiley, Fine-scale prey aggregations and foraging ecology of humpback whales *Megaptera novaeangliae*. *Mar. Ecol. Prog. Ser.* **395**, 75–89 (2009).
46. J. Simmonds, D. N. MacLennan, *Fisheries Acoustics: Theory and Practice* (Blackwell Publishing, Oxford, 2005).
47. J. A. Santora, W. J. Sydeman, I. D. Schroeder, B. K. Wells, J. C. Field, Mesoscale structure and oceanographic determinants of krill hotspots in the California Current: Implications for trophic transfer and conservation. *Prog. Oceanogr.* **91**, 397–409 (2011).

Acknowledgments: For logistical support and assistance in field operations, we thank the captains and crew of the R/V Truth, along with all the scientific personnel from Cascadia and National Oceanic and Atmospheric Administration. Specifically, we want to thank B. Southall and J. Calambokidis for leading the broader experimental design and project management, and S. DeRuiter and A. Stimpert for all their efforts in analyzing tag data. We especially thank D. Nowacek for providing the echo sounder equipment. S. Bograd, B. Sydeman, D. Cade, and M. Jensen all provided useful edits to the manuscript that helped refine it. This study was conducted in accordance with the U.S. National Marine Fisheries Service Permitting authority (permit no. 14534, issued to N. Cyr with B. Southall as chief scientist), the Channel Islands National Marine Sanctuary (permit no. 2010-004, issued to B. Southall), and a consistency determination from the California Coastal Commission. **Funding:** Funding for this study was provided by the U.S. Office of Naval Research (ONR) Marine Mammal Program. The project used ship time funded largely by the U.S. Navy M45 (Environmental Readiness Division) Living Marine Resources Program. **Author contributions:** The experiment was designed by E.L.H. and A.S.F. The data were collected by E.L.H., A.S.F., and J.A.G. and analyzed by E.L.H. and J.A.G. The manuscript was written by E.L.H. and J.A.G. with equal author contributions and edited by A.S.F. **Competing interests:** The authors declare that they have no competing interests. **Data and materials availability:** Data will be made upon request by emailing elliott.hazen@noaa.gov.

Submitted 16 April 2015

Accepted 28 July 2015

Published 2 October 2015

10.1126/sciadv.1500469

Citation: E. L. Hazen, A. S. Friedlaender, J. A. Goldbogen, Blue whales (*Balaenoptera musculus*) optimize foraging efficiency by balancing oxygen use and energy gain as a function of prey density. *Sci. Adv.* **1**, e1500469 (2015).

Blue whales (*Balaenoptera musculus*) optimize foraging efficiency by balancing oxygen use and energy gain as a function of prey density

Elliott Lee Hazen, Ari Seth Friedlaender and Jeremy Arthur Goldbogen

Sci Adv 1 (9), e1500469.
DOI: 10.1126/sciadv.1500469

ARTICLE TOOLS	http://advances.sciencemag.org/content/1/9/e1500469
SUPPLEMENTARY MATERIALS	http://advances.sciencemag.org/content/suppl/2015/09/29/1.9.e1500469.DC1
REFERENCES	This article cites 45 articles, 10 of which you can access for free http://advances.sciencemag.org/content/1/9/e1500469#BIBL
PERMISSIONS	http://www.sciencemag.org/help/reprints-and-permissions

Use of this article is subject to the [Terms of Service](#)